PO Box 2345, Beijing 100023, China
www.wjgnet.com
wjg@wjgnet.com

World J Gastroenterol 2006 October 21; 12(39): 6290-6298
World Journal of Gastroenterology ISSN 1007-9327

LIVER CANCER

Prospective study of differential diagnosis of hepatic tumors by pattern-based classification of contrast-enhanced sonography

Kazushi Numata, Tetsuo Isozaki, Manabu Morimoto, Kazuya Sugimori, Reiko Kunisaki, Toshio Morizane, Katsuaki Tanaka

Kazushi Numata, Tetsuo Isozaki, Manabu Morimoto, Kazuya Sugimori, Reiko Kunisaki, Katsuaki Tanaka, Gastroenterological Center, Yokohama City University Medical Center, Yokohama 232-0024, Japan
Toshio Morizane, Department of Medicine, Kanagawa Dental College, Yokosuka 238-0003, Japan
Correspondence to: Kazushi Numata, MD, Gastroenterological Center, Yokohama City University Medical Center, 4-57 Urafune-cho, Minami-ku, Yokohama 232-0024, Japan. kz-numa@urahp.yokohama-cu.ac.jp
Telephone: +81-45-2615656 Fax: +81-45-2619492
Received: 2006-07-15 Accepted: 2006-07-22

Abstract

AIM: To prospectively evaluate the usefulness of a pattern-based classification of contrast-enhanced sonographic findings for differential diagnosis of hepatic tumors.

METHODS: We evaluated the enhancement pattern of the contrast-enhanced sonography images in 586 patients with 586 hepatic lesions, consisting of 383 hepatocellular carcinomas, 89 metastases, and 114 hemangiomas. After injecting a galactose-palmitic acid contrast agent, lesions were scanned by contrast-enhanced harmonic gray-scale sonography in three phases: arterial, portal, and late. The enhancement patterns of the initial 303 lesions were classified retrospectively, and multiple logistic regression analysis was used to identify enhancement patterns that allowed differentiation between hepatic tumors. We then used the pattern-based classification of enhancement we had retrospectively devised to prospectively diagnose 283 liver tumors.

RESULTS: Seven enhancement patterns were found to be significant predictors of different hepatic tumors. The presence of homogeneous or heterogeneous enhancement both in the arterial and portal phase was the typical enhancement pattern for hepatocellular carcinoma, while the presence of peritumoral vessels in the arterial phase and ring enhancement or a perfusion defect in the portal phase was the typical enhancement pattern for metastases, and the presence of peripheral nodular enhancement both in the arterial and portal phase was the typical enhancement pattern for hemangioma. The sensitivity, specificity, and accuracy of prospective diagnosis based on the combinations of enhancement patterns, respectively, were 93.2%, 96.2%, and 94.0% for hepatocellular carcinoma, 87.9%, 99.6%, and 98.2% for metastasis, and 95.6%, 94.1%, and 94.3% for hemangioma.

CONCLUSION: The pattern-based classification of the contrast-enhanced sonographic findings is useful for differentiating among hepatic tumors.

Key words: Contrast-enhanced sonography; Hepatocellular carcinoma; Metastasis; Hemangioma

Numata K, Isozaki T, Morimoto M, Sugimori K, Kunisaki R, Morizane T, Tanaka K. Prospective study of differential diagnosis of hepatic tumors by pattern-based classification of contrast-enhanced sonography. *World J Gastroenterol* 2006; 12(39): 6290-6298

http://www.wjgnet.com/1007-9327/12/6290.asp

INTRODUCTION

Contrast-enhanced harmonic gray-scale sonography is a useful tool for evaluating the vascularity of liver tumors[1-11], because it allows visualization of the blood perfusion of liver tumors without motion artifacts[12] and it is simple, easy, and sufficiently non-invasive to be performed on an out-patient basis. In addition, it can be used in renal failure patients and patients who are allergic to iodine contrast agents.

Several investigators have reported that contrast-enhanced harmonic gray-scale sonography is a useful modality for differentiating among the types of hepatic tumors. However, no statistical evidence was presented, because they did not use multivariate logistic regression analysis for differential diagnosis of liver tumors[13-22]. We previously classified the contrast-enhanced harmonic gray-scale sonographic findings in hepatic tumors into combinations of enhancement patterns[23]. The results of a multiple logistic regression analysis and positive

predictive values calculated from the results of pattern combinations for each hepatic lesion demonstrated that the enhancement pattern-based classification of contrast-enhanced harmonic gray-scale sonographic findings is useful for making the differential diagnosis of hepatic tumors. However, this classification was not applied to diagnosis prospectively, and a prospective study of the enhancement pattern-based classification was needed to confirm its accuracy for the differential diagnosis for hepatic tumors. Moreover, the perfusion images in our previous study could only be obtained at a slow frame rate, because sufficient time is needed to allow the contrast agent to perfuse the tumor.

In November 2001, we began to use the newly developed contrast-enhanced harmonic gray-scale sonography mode to evaluate tumor vessels and tumor enhancement of hepatic mass lesions. Improvements in spatial and contrast resolution have now made it possible to evaluate the viability of hepatocellular carcinoma at a higher frame rate (7 frames per second) than with the previous mode[23]. Although both the new and previous modes are based on phase inversion technology, by deliberately adjusting the time interval between the transmit pulses, the new contrast mode detects flow motion as well as bubble disruption. This allows the new mode to detect a sufficient flow signal even when there is little contrast agent left in the blood stream. As a result, the new contrast mode enabled identification of hypervascular liver tumors, e.g., advanced hepatocellular carcinoma (HCC) lesions, as hypervascular enhancement in the arterial phase at a high frame rate[11].

In the present study, we first retrospectively classified enhancement pattern combinations for each hepatic lesion obtained with the new contrast mode described above and then prospectively diagnosed each hepatic tumor according to the pattern-based classification of enhancement we had retrospectively devised.

MATERIALS AND METHODS

Patients and tumors in the retrospective evaluation

Between November 2001 and August 2003, we examined 315 consecutive patients with hepatic tumors by conventional sonography. All patients were examined by both dual-phase helical CT and contrast-enhanced harmonic gray-scale sonography, and the patients who were suspected of having HCC were examined by arteriography. Twelve patients with 12 lesions located 12 cm or more beneath the skin surface were excluded, because the increase in attenuation of the ultrasound beam with depth made it difficult to destroy the Levovist bubbles in such lesions[23]. Thus, the remaining 303 patients (238 with solitary focal lesions and 65 with multiple focal lesions) were enrolled in this study, and 303 hepatic lesions were evaluated the largest lesion in patients with more than one focal lesion. Since no significant difference in sensitivity calculated from the results of pattern combinations for each hepatic lesion according to the contrast-enhanced harmonic gray-scale sonographic findings was observed between solitary lesions and multiple lesions in the previous study[23], we enrolled the patients with both solitary and multiple lesions. There were 173 men (104 HCC, 38 metastases, 31 hemangiomas) and 130 women (74 HCC, 18 metastases, 38 hemangiomas), without significant difference in age between the men (65.2 ± 9.6 years) and women (64.4 ± 11.2 years). We classified cholangiocellular carcinoma as hepatic metastasis because pathologically the tumors are adenocarcinomas originating from the intrahepatic bile duct.

The final diagnosis of the lesions studied was HCC in 178 patients, liver metastasis in 56 patients (14 from colon carcinoma, 11 from pancreatic carcinoma, 7 from rectal carcinoma, 6 from cholangiocellular carcinoma, 3 from gastric carcinoma, 3 from gallbladder carcinoma, 2 from malignant melanoma, 2 from lung carcinoma, and 1 each from malignant lymphoma, nasopharyngeal carcinoma, esophageal carcinoma, laryngeal carcinoma, thyroid carcinoma, and hemangiopericytoma), and hemangioma in 69 patients. All HCCs were histologically diagnosed after surgical resection (12 lesions), sonography-guided biopsy (162 lesions), or autopsy (4 lesions). All liver metastases were histologically diagnosed after surgical resection (6 lesions), sonography-guided biopsy (48 lesions), and autopsy (2 lesions). The diagnosis of hemangioma was confirmed by contrast-enhanced CT and MR and the absence of any changes on follow-up images more than 1 year later. Of the 178 patients with HCC lesions, 155 had cirrhosis, and the diagnosis was made histologically and/or clinically.

The hepatic tumors were measured on conventional US images by one of the two operators who performed the contrast-enhanced harmonic imaging. The mean maximal diameters were: 26 ± 16 mm for HCCs, 33 ± 21 mm for metastases, and 28 ± 19 mm for hemangiomas. The numbers of HCC lesions, classified according to maximal tumor diameter, were 2 lesions < 10 mm, 87 lesions between 10 mm and 20 mm, and 89 lesions > 20 mm.

Patients and tumors in the prospective evaluation

Between September 2003 and April 2005, we examined 283 consecutive patients (195 men with age 67.1 ± 9.2 years, and 88 women with age 68.0 ± 8.8 years) with hepatic tumors by conventional US, and using the pattern-based classification of enhancement, we retrospectively devised to prospectively diagnose their liver tumors. Solitary focal lesions were detected in 207 patients and multiple focal lesions in 76 patients.

The final diagnosis of the lesions was HCC in 205 patients, liver metastasis in 33 patients (8 from colon carcinoma, 8 cholangiocellular carcinoma, 4 from pancreatic carcinoma, 4 from gastric carcinoma, 2 from gallbladder carcinoma and 1 each from esophageal carcinoma, lung carcinoma, rectal carcinoma, prostate carcinoma, malignant lymphoma, adenoid cystic carcinoma, and leiomyosarcoma), and hemangioma in 45. All liver metastases were histologically diagnosed after surgical resection (5 lesions), sonography-guided biopsy (27 lesions), and autopsy (1 lesion). Of the 205 HCC lesions, 12 were histologically diagnosed after resection, 194 after sonography-guided biopsy, and the remaining 3 after autopsy. Of the 205 patients with HCC lesions, 177 had cirrhosis which was diagnosed histologically and/or

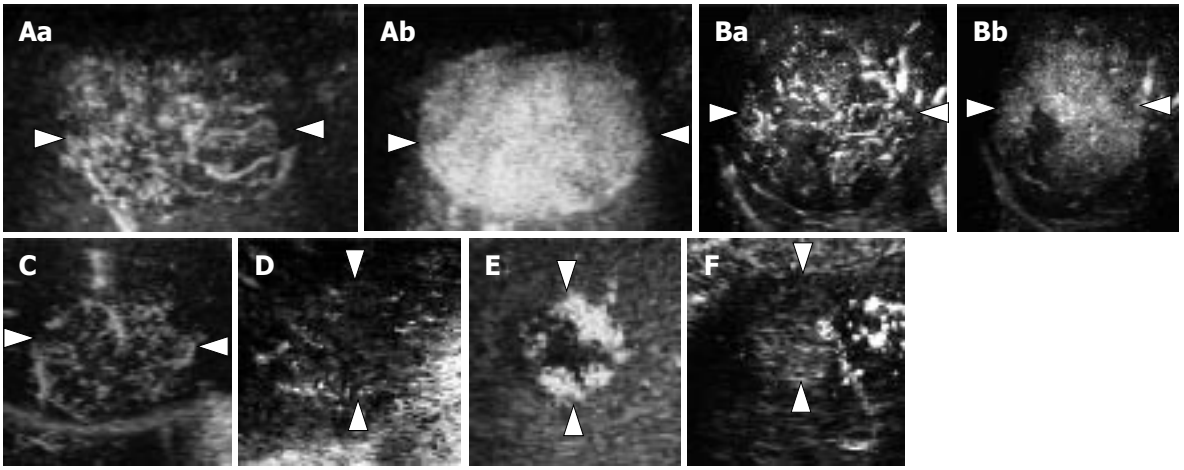

Figure 1 Diagram showing enhancement patterns of hepatic tumors in the arterial phase. **A**: Intratumoral vessels in the early arterial phase (a) with homogeneous enhancement in the late arterial phase (b) (pattern A1); **B**: Intratumoral vessels in the early arterial phase (a) with heterogeneous enhancement in the late arterial phase (b) (pattern A1); **C**: Intratumoral vessels without homogeneous or heterogeneous enhancement (pattern A2); **D**: Peritumoral vessels alone (pattern A3); **E**: Peripheral nodular enhancement without tumor vessels (pattern A4); **F**: No enhancement and no tumor vessels (pattern A5).

clinically.

The hepatic tumors were measured by conventional US by one of the two operators who performed the contrast-enhanced harmonic imaging. The mean maximal diameter of the HCCs was 26 ± 15 mm, of the metastases was 33 ± 17 mm, and of the hemangiomas was 30 ± 22 mm.

Informed consent was obtained from all patients before the study, and the study was approved by Institutional Ethics Committee.

We defined "early HCC lesions" as well-differentiated cancers with no substantial destruction of the preexisting hepatic framework[24].

Procedures

To minimize variations between operators, the contrast-enhanced harmonic gray-scale imaging studies were performed by either one of two operators (K. N., T. I.) using the same examination protocol. Neither operator was aware of the results of the helical CT and angiography examinations or the histological diagnosis. Contrast-enhanced harmonic gray-scale sonography was performed with a SONOLINE Elegra machine (Siemens Medical Systems, Issaquah, WA), a 3.5-MHz convex probe, and Sie flow mode imaging software until the end of September 2004, and with a LOGIQ 7 machine (GE Healthcare, Milwaukee, WI), a 3.5-MHz convex probe, and Coded harmonic angio mode imaging software from October 2004 onward.

After intravenous bolus injection of a half vial of the 300 mg/mL concentration of galactose–palmitic acid mixture contrast medium (Levovist; Schering AG, Berlin, Germany), the liver was scanned by real-time contrast-enhanced harmonic gray-scale sonography at 5-13 frames per second, usually at 7 frames per second. The transmission power was 100%, and the mechanical index values were between 1.0 and 1.6. The focus position was just below the bottom of the tumor. Levovist is a suspension of galactose (99.9%) stabilized with 0.1% palmitic acid. A 3.5-mL dose of this agent was injected at 0.5 mL/s *via* a 22-gauge cannula placed in an antecubital vein. After the bolus injection of Levovist, 50 g/L glucose was continuously infused at 5 mL/min. The patients gently inspired and then held their breath for about 30 s (10-40 s after the contrast medium injection) while the tumor vessels and tumor enhancement were examined (arterial phase).

After observation of the arterial phase, we froze the image. In the cases scanned with the Elegra machine, we reviewed the images frame by frame from cine loop memories and stored them on magneto-optical disks. In the cases scanned with the LOGIQ 7 machine, we stored the images as a cine clip with GE exclusive raw-data format files in the LOGIQ 7 computer. This procedure took approximately 15-35 s (mean, 25 s), and we used the time to allow the contrast agent to pool in the hepatic parenchyma. We then scanned the whole tumor and examined the tumor for enhancement 60-120 s after injection of the contrast agent while the patients held their breath for a few seconds (portal phase). We froze the images and stored them by the same method as mentioned above. Finally, 5 min after injection of the contrast agent, we examined the lesion in a sweep scan to determine if it was iso-echoic or hypo-echoic (late phase). We stored these images by the same method as described above. The complete examinations were recorded on S-VHS videotape.

Image evaluation

We evaluated the images for the presence and shape of tumor vessels and the enhancement patterns during the arterial phase and classified the patterns into five categories (Figure 1) as follows: pattern A1, intratumoral vessels with homogeneous (Figure 1A) or heterogeneous enhancement (Figure 1B); pattern A2, intratumoral vessels without homogeneous or heterogeneous enhancement (Figure 1C); pattern A3, peritumoral vessels alone (Figure 1D); pattern A4, peripheral nodular enhancement without tumor vessels (Figure 1E); and pattern A5, no enhancement

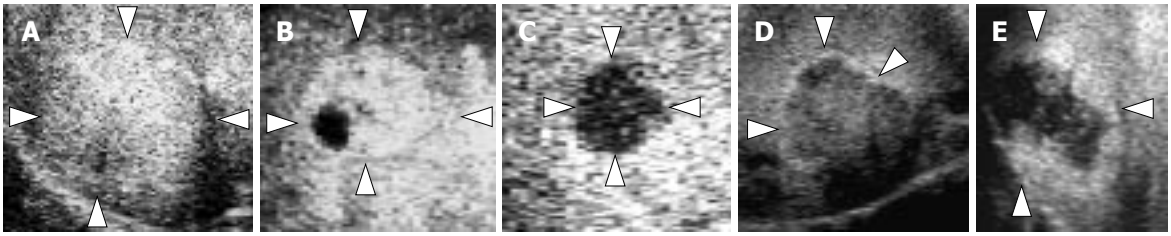

Figure 2 Diagram showing enhancement patterns of hepatic tumors in the portal phase. **A**: Homogeneous enhancement (pattern P1); **B**: Heterogeneous enhancement (pattern P1); **C**: Perfusion defect (pattern P2); **D**: Ring enhancement (pattern P3); **E**: Peripheral nodular enhancement (pattern P4).

and no tumor vessels (Figure 1F). In the portal phase, the enhancement patterns of the lesions were classified into four categories (Figure 2) as follows: pattern P1, homogeneous (Figure 2A) or heterogeneous enhancement (Figure 2B); pattern P2, perfusion defect (Figure 2C); pattern P3, ring enhancement (Figure 2D); and pattern P4, peripheral nodular enhancement (Figure 2E). The enhancement patterns of the lesion in the late phase were classified into two categories relative to the enhancement pattern in the surrounding liver parenchyma (Figure 3): pattern L1, iso-echoic (Figure 3A); and pattern L2, hypo-echoic (Figure 3B).

The image evaluation was performed independently by two readers (K.T., M.M.), both of whom reviewed all of the sonographic images recorded on video-tape, cine clips, and magneto-optical disks, and they were asked to classify each lesion into one of the patterns shown in Figures 1-3. The readers had no knowledge of the results of the helical CT or angiography, or of the histological diagnosis. Since 16 of the 586 hepatic lesions were classified differently by the two readers, the two readers and the two operators had a consensus meeting to arrive at a consensus for the final classification.

Statistical analysis

A multiple logistic regression analysis was performed to select independent variables of imaging features associated with the dependent variable, i.e., tumor type, as described previously[23]. Since only dichotomous variables can be used as the dependent variable in multiple logistic regression analyses, we used one of the three tumor types *versus* the other two tumor types as the dependent variables in our analysis. The independent variables were different imaging features observed in the three different phases after contrast enhancement, and each variable had a dichotomous value (not observed = 0, observed = 1). We selected independent variables with a P value less than 0.05 in the multiple logistic regression analysis and used these significant independent variables to construct a multivariable model. All tumors exhibited one of the defined combinations of statistically significant independent variables, and statistically significant independent variables were used to make the defined combinations. The diagnostic performance of our multivariable model was evaluated by calculating the positive predictive values according to Bayes theorem[25], based on sensitivity, specificity, and prior probability (positive predictive values = prior probability × sensitivity/{sensitivity × prior probability + (1-specificity) × (1- prior probability)}). Prior probability was calculated by dividing the numbers of HCCs, metastases, and hemangiomas by the total number of tumors (303 tumors). The diagnosis of each hepatic tumor was made on the basis of the largest positive predictive value of each combined enhancement pattern based on the results of the retrospective study, and the enhancement patterns of the prospective study were used to make the diagnosis based on the results of the retrospective study. Finally, we calculated the sensitivity, specificity, and accuracy of each tumor diagnosis based on the results of the enhancement pattern-based classification system as described above. The SPSS computer program (SPSS Japan, Tokyo, Japan) was used to perform the data analysis.

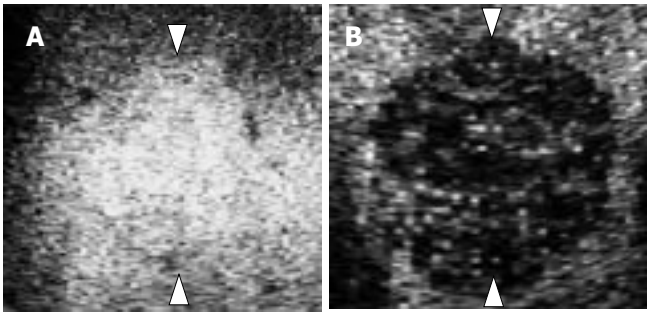

Figure 3 Diagram showing enhancement patterns of hepatic tumors in the late phase. **A**: Lso-echoic (pattern L1); **B**: Hypo-echoic (pattern L2).

RESULTS

Retrospective study

Arterial phase: Table 1 shows the enhancement patterns of hepatic tumors observed by contrast-enhanced harmonic gray-scale sonography. In the arterial phase, 169 (95%) of the 178 HCC lesions showed intratumoral vessels with homogeneous or heterogeneous enhancement (pattern A1), and among the other 9 HCC lesions, 1 (1%) showed intratumoral vessels without homogeneous or heterogeneous enhancement (pattern A2), 2 (1%) showed a peripheral nodular enhancement without tumor vessels (pattern A4), and 6 (3%) showed no enhancement and no tumor vessels (pattern A5). Five (9%) of the 56 liver metastases showed intratumoral vessels with homogeneous or heterogeneous enhancement (pattern A1), 15 (27%) showed intratumoral vessels without

Table 1 Retrospective study of enhancement patterns of hepatic tumors

	Hepatocellular carcinoma *n* = 178	Metastasis *n* = 56	Hemangioma *n* = 69
Arterial phase			
A1	95% (169/178)	9% (5/56)	0% (0/69)
A2	1% (1/178)	27% (15/56)	1% (1/69)
A3	0% (0/178)	55% (31/56)	0% (0/69)
A4	1% (2/178)	0% (0/56)	61% (42/69)
A5	3% (6/178)	9% (5/56)	38% (26/69)
Portal phase			
P1	93% (166/178)	16% (9/56)	46% (32/69)
P2	4% (8/178)	14% (8/56)	0% (0/69)
P3	1% (2/178)	66% (37/56)	1% (1/69)
P4	1% (2/178)	4% (2/56)	52% (36/69)
Late Phase			
L1	8% (14/178)	0% (0/56)	20% (14/69)
L2	92% (164/178)	100% (56/56)	80% (55/69)

A1: Intratumoral vessels with homogeneous or heterogeneous enhancement; A2: Intratumoral vessels without homogeneous or heterogeneous enhancement; A3: Peritumoral vessels; A4: Peripheral nodular enhancement without tumor vessels; A5: No enhancement and no tumor vessels; P1: Homogeneous or heterogeneous enhancement; P2: Perfusion defect; P3: Ring enhancement; P4: Peripheral nodular enhancement; L1: Iso-echoic; L2: Hypo-echoic.

homogeneous or heterogeneous enhancement (pattern A2), 31 (55%) showed peritumoral vessels (pattern A3), and 5 (9%) showed no enhancement and no tumor vessels (pattern A5). One (1%) of the 69 hemangiomas showed intratumoral vessels without homogeneous or heterogeneous enhancement (pattern A2), 42 showed peripheral nodular enhancement without tumor vessels in the arterial phase (pattern A4), and 26 (38%) showed no enhancement and no tumor vessels (pattern A5).

Portal phase: In the portal phase, 166 (93%) of the 178 HCC lesions showed a homogeneous or heterogeneous pattern of enhancement (pattern P1): a homogeneous pattern in 148 (83%), and a heterogeneous pattern in 18 (10%). Since Levovist did not enhance the necrotic areas of the tumors, tumors that contained necrotic areas showed a heterogeneous pattern[23]. Eight (4%) of the 178 lesions showed a perfusion defect in the portal phase (pattern P2): two exhibited arterioportal shunting on arteriography and intratumoral vessels with homogeneous enhancement in the arterial phase, and the remaining 6 lesions were early HCCs. Two (1%) of the remaining 4 (2%) HCC lesions showed ring enhancement (pattern P3) and 2 (1%) showed a peripheral nodular enhancement (pattern P4). Nine (16%) of the 56 liver metastases showed homogeneous or heterogeneous enhancement (pattern P1), 8 (14%) showed a perfusion defect (pattern P2), 37 (66%) showed ring enhancement (pattern P3), and 2 (4%) showed peripheral nodular enhancement (pattern P4). Of the 69 hemangiomas, 32 (46%) showed homogeneous enhancement (pattern P1), 1 (1%) showed ring enhancement (pattern P3), and 36 (52%) showed peripheral nodular enhancement (pattern P4).

Late phase: In the late phase, 164 (92%) of the HCC lesions were visualized as hypo-echoic with the surrounding liver parenchyma (pattern L1), and 14 (8%) as iso-echoic (pattern L2). Histological examination revealed that all iso-echoic HCCs lesions in the late phase were well differentiated HCCs. All metastases were hypo-echoic (pattern L1). Of the 69 hemangiomas, 55 (80%) were hypo-echoic (pattern L1), and the remaining14 (20%) were iso-echoic (pattern L2).

Table 2 Logistic regression analyses for the diagnosis of hepatocellular carcinoma, metastasis, and hemangioma

	Odds ratio	95% CI	*P*
Hepatocellular carcinoma			
A1	189.665	25.716-1398.871	< 0.01
P1	38.993	4.616-329.381	< 0.01
Metastases			
A3	73.139	7.19-743.997	< 0.01
P2	27.973	5.202-150.421	< 0.01
P3	137.385	27.064-697.421	< 0.01
Hemangioma			
A4	102.175	15.567-670.619	< 0.01
P4	695.141	110.903-4357.157	< 0.01

A1: Intratumoral vessels with homogeneous or heterogeneous enhancement; A3: Peritumoral vessels; A4: Peripheral nodular enhancement without tumor vessels; P1: Homogeneous or heterogeneous enhancement; P2: Perfusion defect; P3: Ring enhancement; P4: Peripheral nodular enhancement.

Factors predicting the diagnosis of hepatic tumors: To identify predictors of the diagnosis of hepatic tumors, multiple logistic regression analysis was performed on 11 parameters based on the results of contrast-enhanced harmonic gray-scale sonography with contrast agents. Only 7 parameters were selected as independent variables associated with a type of hepatic tumor (Table 2). Intratumoral vessels with homogeneous or heterogeneous enhancement in the arterial phase (pattern A1) (odds ratio: 189.665; $P < 0.01$) and homogeneous or heterogeneous enhancement in the portal phase (pattern P1) (odds ratio: 38.993; $P < 0.01$) were selected as statistically significant variables to differentiate HCC from the other two types of hepatic lesions combined, i.e., metastases and hemangiomas. Peritumoral vessels in the arterial phase (pattern A3) (odds ratio: 73.139; $P < 0.01$), perfusion defect in the portal phase (pattern P2) (odds ratio: 17.92; $P < 0.01$), and ring enhancement in the portal phase (pattern P3) (odds ratio: 137.385; $P < 0.01$) were selected as statistically significant variables to differentiate metastases from the other two types of lesions combined, i.e., HCCs and hemangiomas. Peripheral nodular enhancement without tumor vessels in the arterial phase (pattern A4) (odds ratio: 102.175; $P < 0.01$) and peripheral nodular enhancement in the portal phase (pattern P4) (odds ratio: 695.141; $P < 0.01$) were selected as statistically significant variables to differentiate hemangiomas from the other two types of lesions combined, i.e., HCCs and metastases. Two parameters of the late phase were not statistically significant variables.

Enhancement pattern-based classification: Combinations of patterns of enhancement in the arterial phase (A1, A3, A4, and others) and portal phase (P1, P2, P3, and

Table 3 Enhancement pattern-based classification of contrast-enhanced harmonic gray-scale sonography images and positive predictive value for differentiating hepatic tumors

Enhancement pattern			Positive predictive value (No. of lesions)			Diagnosis[1]
Pattern combination	Arterial phase	Portal phase	HCC (n = 178)	Metastasis (n = 56)	Hemangioma (n = 69)	
1	A1	P1	0.996 (165)	0.004 (2)	0 (0)	HCC
2	A1	P2	1 (2)	0 (0)	0 (0)	HCC
3	A1	P3	0 (0)	1 (3)	0 (0)	Metastasis
4	A1	P4	1 (2)	0 (0)	0 (0)	HCC
5	A3	P1	0 (0)	1 (4)	0 (0)	Metastasis
6	A3	P2	0 (0)	1 (3)	0 (0)	Metastasis
7	A3	P3	0 (0)	1 (24)	0 (0)	Metastasis
8	A4	P1	0 (0)	0 (0)	1 (25)	Hemangioma
9	A4	P3	0.84 (2)	0 (0)	0.16 (1)	HCC
10	A4	P4	0 (0)	0 (0)	1 (16)	Hemangioma
11	others[2]	P1	0.20 (1)	0.19 (3)	0.61(8)	Hemangioma
12	others[2]	P2	0.79 (6)	0.21 (5)	0 (0)	HCC
13	others[2]	P3	0 (0)	1 (11)	0 (0)	Metastasis
14	others[2]	P4	0 (0)	0.04 (1)	0.96 (19)	Hemangioma

A1: Intratumoral vessels with homogeneous or heterogeneous enhancement; A3: Peritumoral vessels; A4: Peripheral nodular enhancement without tumor vessels; P1: homogeneous or heterogeneous enhancement; P2: Perfusion defect; P3: Ring enhancement; P4: Peripheral nodular enhancement. [1]Diagnosis was made on the basis of the largest positive predictive value for each of the three kinds of tumors in each combination of enhancement patterns. [2]Others mean A2 or A5 as shown in Table 1.

Table 4 Prospective study of pattern combination-based classification of contrast-enhanced harmonic gray-scale sonography images for differentiating hepatic tumors

Enhancement pattern			No. of lesions			Diagnosis[1]
Pattern combination	Arterial phase	Portal phase	HCC (n = 205)	Metastasis (n = 33)	Hemangioma (n = 45)[2]	
1	A1	P1	183	3	0	HCC
2	A1	P2	0	0	0	HCC
3	A1	P3	0	5	0	Metastasis
4	A1	P4	0	0	0	HCC
5	A3	P1	0	1	1	Metastasis
6	A3	P2	0	1	0	Metastasis
7	A3	P3	0	14	0	Metastasis
8	A4	P1	0	0	16	Hemangioma
9	A4	P3	0	0	0	HCC
10	A4	P4	0	0	7	Hemangioma
11	Others[3]	P1	14	1	2	Hemangioma
12	Others[3]	P2	8	0	0	HCC
13	Others[3]	P3	0	8	0	Metastasis
14	Others[3]	P4	0	0	18	Hemangioma

A1: Intratumoral vessels with homogeneous or heterogeneous enhancement; A3: Peritumoral vessels; A4: Peripheral nodular enhancement without tumor vessels; P1: Homogeneous or heterogeneous enhancement; P2: Perfusion defect; P3: Ring enhancement; P4: Peripheral nodular enhancement. [1]Diagnosis was made on the basis of the largest positive predictive value for each of the three kinds of tumors in each combination of enhancement patterns in the retrospective study. [2]One case of hemangioma was not diagnosed because the pattern combination did not exist in Table 3. [3]Others mean A2 or A5 as shown in Table 1.

P4) were then analyzed, and 16 different combinations of statistically significant predictors in the arterial phase and portal phase were identified. Since two combinations of patterns were not observed in any of the cases in this study, only 14 patterns were analyzed (Table 3).

Enhancement pattern combinations 1, 2, 4, 9, and 12 showed high positive predictive value for HCC, and "pattern combination 1" was the most predominant pattern among them. According to the greatest tumor diameter, the numbers of all lesions that were "pattern combination 1" lesions were: 2 (100%) of 2 lesions less than 10 mm; 82 (94%) of 87 lesions between 10 and 20 mm; and 81 (91%) of 89 lesions greater than 20 mm. Both "pattern combination 2" lesions were HCCs with arterioportal shunting. Five of the six "pattern combination 12" lesions were early HCCs.

The enhancement pattern combinations 3, 5, 6, 7, and 13 showed high positive predictive value for metastasis, and "pattern combination 7" was the predominant pattern. "Pattern combinations 3 and 13" were observed in hypervascular metastases.

Enhancement "pattern combinations 8, 10, 11, and 14" showed high positive predictive value for hemangioma, and "pattern combination 8" was the most predominant pattern among them. The hemangiomas that showed "pattern combination 8" were relatively high-flow type hemangiomas. All 8 lesions that showed "pattern combination 11" exhibited no enhancement and no tumor vessels in the arterial phase, and homogeneous enhancement in the portal phase.

Prospective study

Table 4 shows the results of a prospective study of hepatic tumors diagnosed by using the pattern combination-based classification of the contrast-enhanced harmonic gray-scale sonography findings. Three combination patterns were not found in any of the cases in the prospective study.

Of the 205 HCCs, 183 lesions corresponded to "pattern combination 1", and 8 corresponded to "pattern combination 12"; these lesions were correctly diagnosed as HCC. According to greatest tumor diameter, the numbers of all lesions that were "pattern combination 1" were: 1 (50%) of 2 lesions less than 10 mm; 80 (83%) of 96 lesions between 10 mm and 20 mm; and 102 (95%) of 107 lesions greater than 20 mm. Fourteen HCC lesions were not diagnosed as HCC. These lesions were corresponded to "pattern combination 11" and were diagnosed as hemangioma. Eleven of the 14 "pattern combination 11" lesions showed intratumoral vessels without homogeneous or heterogeneous enhancement in the arterial phase (pattern A2), and the remaining three showed no enhancement and no tumor vessels in the arterial phase (pattern A5). These lesions were histologically diagnosed as well differentiated HCC.

Of the 33 metastases, 14 corresponded to "pattern combination 7", 8 to "pattern combination 13", 5 to "pattern combination 3", and one each to "pattern combinations 5 and 6". These 29 lesions were correctly diagnosed as metastases. Four metastases were not diagnosed as metastases; three corresponding to "pattern

combination 1" were diagnosed as HCC, and one corresponding to "pattern combination 11" was diagnosed as hemangioma.

Of the 45 hemangiomas, 16 corresponded to "pattern combination 8", 7 to "pattern combination 10", 18 to "pattern combination 14", and 2 to "pattern combination 11". These hemangioma lesions were not correctly diagnosed as hemangiomas. One hemangioma was not diagnosed as hemangioma; it corresponded to "pattern combination 5" and was diagnosed as a metastasis. The remaining one case of hemangioma was not diagnosed because the pattern combination did not exist in the retrospective study.

The sensitivity, specificity, and accuracy of prospective diagnosis based on the combinations of enhancement patterns, respectively, were 93.2%, 96.2%, and 94.0% for hepatocellular carcinoma, 87.9%, 99.6%, and 98.2% for metastasis, and 95.6%, 94.1%, and 94.3% for hemangioma.

DISCUSSION

In the present study, we first retrospectively classified the contrast-enhanced harmonic gray-scale sonography findings in hepatic tumors into combinations of enhancement patterns. The results of a multiple logistic regression analysis and the positive predictive values calculated from the results of the pattern combinations for each hepatic lesion demonstrated that the enhancement pattern-based classification of contrast-enhanced harmonic gray-scale sonography findings was useful for making the differential diagnosis of hepatic tumors in the subsequent prospective study. Hence, we concluded that contrast-enhanced harmonic gray-scale sonography is a useful modality for differentiating among the types of hepatic tumors we studied.

To visualize tumor perfusion in our previous mode of contrast-enhanced harmonic gray-scale sonography, we reduced bubble destruction and used a frame rate of 2 frames per second, and at that rate intratumoral vessels were observed in the arterial phase in 98 (84%) of the 116 lesions[23]. We used the novel mode in the present study and 169 (95%) of the 178 hepatocellular carcinoma lesions showed homogeneous or heterogeneous enhancement with intratumoral vessels in the arterial phase. Clearer and more frequent visualizations of homogeneous or heterogeneous enhancement with intratumoral vessels were achieved when the frame rate was 7 frames per second. This real-time observation of the arterial phase made the diagnosis of hepatocellular carcinoma easier when the lesion showed hypervascular enhancement with intratumoral vessels. This novel mode of real-time contrast-enhanced harmonic gray-scale sonography also enabled detection of viable hepatocellular carcinoma lesions which were not detected by conventional sonography[11], and we were able to treat these lesions in real time by percutaneous therapy under guidance by this modality. Improved sensitivity also permitted us to perform this examination after injection of a smaller volume of contrast agent than with the previous mode[11].

The arteries feeding hepatic tumors are directly supplied by branches of the hepatic artery. Hemangiomas are hypervascular tumors in which normal-caliber arteries taper normally and subdivide normally into small vessels[26]. The typical finding of hemangiomas in previous mode was absence of enhancement in the arterial phase[23]. However, the typical findings of hemangioma in the present study were peripheral nodular enhancement without tumor vessels in the arterial phase of contrast-enhanced harmonic gray-scale sonography. The novel contrast mode improved both spatial resolution and contrast resolution, and this development made it possible to observe peripheral nodular enhancement in the arterial phase. The arterial branches supplying HCCs tend to show irregularly tortuous extension, whereas the arterial branches supplying hepatic metastases are scanty or fine, and are located in the periphery of the tumors, distinguishing them from HCCs[27]. The typical arterial phase finding in metastases is peritumoral vessels without early enhancement, whereas the typical finding in HCCs is intratumoral vessels with homogeneous or heterogeneous enhancement. These different findings in the arterial phase may be of use in differentiating between hypervascular metastasis and typical HCC. Moreover, more than 80% of metastases show ring enhancement or a perfusion defect in the portal phase, whereas more than 95% of HCCs show homogeneous or heterogeneous enhancement in the portal phase. However, the tumor vessels of hepatic metastases exhibit many variations. Hypervascular metastases sometimes show intratumoral vessels with homogeneous or heterogeneous enhancement in the arterial phase, and this enhancement pattern mimics that of HCC. In the portal phase, however, almost all hypervascular metastases showed ring enhancement. Thus, the combinations of pattern enhancement in the arterial and the portal phase are useful for making the differential diagnosis of hepatic tumors.

The multivariate analysis in the present study showed that the parameters in the late phase were not significant predictors of the diagnosis, suggesting that observation of the vascular phase (arterial and portal phase) is important in making the differential diagnosis of hepatic tumors. This finding is the same as with the previous mode[23]. We think that the late phase may be useful for detecting metastases, because all metastases were visualized as a hypo-echoic lesion in the late phase. All HCC lesions that exhibited "pattern combination 1" in the vascular phase and that were iso-echoic in the late phase were well differentiated HCC, whereas almost all HCC lesions with "pattern combination 1" in the vascular phase and hypo-echoic in the late phase were moderately to poorly differentiated HCC. These results are similar to those reported by Nicolau *et al*[28] in a study using SonoVue, a second generation ultrasound contrast agent. We think that the late phase finding may be useful for evaluating the grade of malignancy of HCC. However, they are not of value for differentiating hepatic tumors, because whether a lesion is iso-echoic or hypo-echoic with the surrounding liver parenchyma is not a significant predictor of the diagnoses of hepatic tumors.

In this prospective study, the pattern-based classification failed to correctly diagnose 14 HCC lesions that were histologically well differentiated HCCs. These lesions

did not show early homogeneous or heterogeneous enhancement in the arterial phase, but showed homogeneous or heterogeneous enhancement in the portal phase. These misdiagnoses are attributable to the fact that there were only a small number of well differentiated HCC lesions in the retrospective study compared to the prospective study, because 1 HCC lesion, 3 metastatic lesions, and 8 hemangioma lesions exhibited this pattern of enhancement in the retrospective study and it had high positive predictive value for hemangioma.

The European Association for the Study of the Liver (EASL) conference has stated that HCC can be diagnosed without biopsy in patients with cirrhosis who have a lesion greater than 2 cm in diameter that shows characteristic arterial vascularization on two different imaging modalities, i.e., triphasic CT scan and MRI[29,30]. Such lesions should be treated as HCC, since the positive predictive value of the clinical and radiological findings exceeds 95%[29,30]. In this study, 348 (93%) of the 379 HCC lesions equal to or greater than 10 mm exhibited the most predominant pattern of HCC lesions on contrast-enhanced sonography. Because contrast-enhanced sonography has highly accuracy for the diagnosis of HCC, we hope that this modality will be included in imaging modalities like triphasic CT scan and MRI.

We prospectively diagnosed hepatic tumors correctly according to the results of the enhancement pattern based on the retrospective study using Levovist, a first-generation contrast agent, suggesting that this enhancement pattern-based classification will be useful for differentiating among the hepatic tumors in future trials using second-generation contrast agents.

REFERENCES

1 **Blomley MJ**, Albrecht T, Cosgrove DO, Patel N, Jayaram V, Butler-Barnes J, Eckersley RJ, Bauer A, Schlief R. Improved imaging of liver metastases with stimulated acoustic emission in the late phase of enhancement with the US contrast agent SH U 508A: early experience. *Radiology* 1999; **210**: 409-416

2 **Wilson SR**, Burns PN, Muradali D, Wilson JA, Lai X. Harmonic hepatic US with microbubble contrast agent: initial experience showing improved characterization of hemangioma, hepatocellular carcinoma, and metastasis. *Radiology* 2000; **215**: 153-161

3 **Kim TK**, Choi BI, Han JK, Hong HS, Park SH, Moon SG. Hepatic tumors: contrast agent-enhancement patterns with pulse-inversion harmonic US. *Radiology* 2000; **216**: 411-417

4 **Burns PN**, Wilson SR, Simpson DH. Pulse inversion imaging of liver blood flow: improved method for characterizing focal masses with microbubble contrast. *Invest Radiol* 2000; **35**: 58-71

5 **Numata K**, Tanaka K, Kiba T, Saito S, Ikeda M, Hara K, Tanaka N, Morimoto M, Iwase S, Sekihara H. Contrast-enhanced, wide-band harmonic gray scale imaging of hepatocellular carcinoma: correlation with helical computed tomographic findings. *J Ultrasound Med* 2001; **20**: 89-98

6 **Ding H**, Kudo M, Onda H, Suetomi Y, Minami Y, Chung H, Kawasaki T, Maekawa K. Evaluation of posttreatment response of hepatocellular carcinoma with contrast-enhanced coded phase-inversion harmonic US: comparison with dynamic CT. *Radiology* 2001; **221**: 721-730

7 **Tanaka S**, Ioka T, Oshikawa O, Hamada Y, Yoshioka F. Dynamic sonography of hepatic tumors. *AJR Am J Roentgenol* 2001; **177**: 799-805

8 **Numata K**, Tanaka K, Kiba T, Saito S, Isozaki T, Hara K, Morimoto M, Sekihara H, Yonezawa H, Kubota T. Using contrast-enhanced sonography to assess the effectiveness of transcatheter arterial embolization for hepatocellular carcinoma. *AJR Am J Roentgenol* 2001; **176**: 1199-1205

9 **Albrecht T**, Hoffmann CW, Schmitz SA, Schettler S, Overberg A, Germer CT, Wolf KJ. Phase-inversion sonography during the liver-specific late phase of contrast enhancement: improved detection of liver metastases. *AJR Am J Roentgenol* 2001; **176**: 1191-1198

10 **Dill-Macky MJ**, Burns PN, Khalili K, Wilson SR. Focal hepatic masses: enhancement patterns with SH U 508A and pulse-inversion US. *Radiology* 2002; **222**: 95-102

11 **Numata K**, Isozaki T, Ozawa Y, Sakaguchi T, Kiba T, Kubota T, Ito A, Sugimori K, Shirato K, Morimoto M, Tanaka K. Percutaneous ablation therapy guided by contrast-enhanced sonography for patients with hepatocellular carcinoma. *AJR Am J Roentgenol* 2003; **180**: 143-149

12 **Correas JM**, Bridal L, Lesavre A, Méjean A, Claudon M, Hélénon O. Ultrasound contrast agents: properties, principles of action, tolerance, and artifacts. *Eur Radiol* 2001; **11**: 1316-1328

13 **Kim EA**, Yoon KH, Lee YH, Kim HW, Juhng SK, Won JJ. Focal hepatic lesions: contrast-enhancement patterns at pulse-inversion harmonic US using a microbubble contrast agent. *Korean J Radiol* 2003; **4**: 224-233

14 **Wen YL**, Kudo M, Zheng RQ, Ding H, Zhou P, Minami Y, Chung H, Kitano M, Kawasaki T, Maekawa K. Characterization of hepatic tumors: value of contrast-enhanced coded phase-inversion harmonic angio. *AJR Am J Roentgenol* 2004; **182**: 1019-1026

15 **Dietrich CF**, Ignee A, Trojan J, Fellbaum C, Schuessler G. Improved characterisation of histologically proven liver tumours by contrast enhanced ultrasonography during the portal venous and specific late phase of SHU 508A. *Gut* 2004; **53**: 401-405

16 **Luo BM**, Wen YL, Yang HY, Zhi H, Ou B, Ma JH, Pan JS, Dai XN. Differentiation between malignant and benign nodules in the liver: use of contrast C3-MODE technology. *World J Gastroenterol* 2005; **11**: 2402-2407

17 **von Herbay A**, Vogt C, Willers R, Häussinger D. Real-time imaging with the sonographic contrast agent SonoVue: differentiation between benign and malignant hepatic lesions. *J Ultrasound Med* 2004; **23**: 1557-1568

18 **Quaia E**, Calliada F, Bertolotto M, Rossi S, Garioni L, Rosa L, Pozzi-Mucelli R. Characterization of focal liver lesions with contrast-specific US modes and a sulfur hexafluoride-filled microbubble contrast agent: diagnostic performance and confidence. *Radiology* 2004; **232**: 420-430

19 **Peschl R**, Werle A, Mathis G. Differential diagnosis of focal liver lesions in signal-enhanced ultrasound using BR 1, a second-generation ultrasound signal enhancer. *Dig Dis* 2004; **22**: 73-80

20 **Brannigan M**, Burns PN, Wilson SR. Blood flow patterns in focal liver lesions at microbubble-enhanced US. *Radiographics* 2004**; 24**: 921-935

21 **Ding H**, Wang WP, Huang BJ, Wei RX, He NA, Qi Q, Li CL. Imaging of focal liver lesions: low-mechanical-index real-time ultrasonography with SonoVue. *J Ultrasound Med* 2005; **24**: 285-297

22 **Wilson SR**, Burns PN. An algorithm for the diagnosis of focal liver masses using microbubble contrast-enhanced pulse-inversion sonography. *AJR Am J Roentgenol* 2006; **186**: 1401-1412

23 **Isozaki T**, Numata K, Kiba T, Hara K, Morimoto M, Sakaguchi T, Sekihara H, Kubota T, Shimada H, Morizane T, Tanaka K. Differential diagnosis of hepatic tumors by using contrast enhancement patterns at US. *Radiology* 2003; **229**: 798-805

24 **Kanai T**, Hirohashi S, Upton MP, Noguchi M, Kishi K, Makuuchi M, Yamasaki S, Hasegawa H, Takayasu K, Moriyama N. Pathology of small hepatocellular carcinoma. A proposal for a new gross classification. *Cancer* 1987; **60**: 810-819

25 **Degoulet P**, Fieschi M. Medical decision support systems. In: Degoulet P, Fieschi M eds. Introduction to clinical informatics. New York: Springer-Verlag, 1997: 153-168

26 **McLoughlin MJ**. Angiography in cavernous hemangioma

of the liver. *Am J Roentgenol Radium Ther Nucl Med* 1971; **113**: 50-55
27 **Kido C**, Sasaki T, Kaneko M. Angiography of primary liver cancer. *Am J Roentgenol Radium Ther Nucl Med* 1971; **113**: 70-81
28 **Nicolau C**, Catalá V, Vilana R, Gilabert R, Bianchi L, Solé M, Pagés M, Brú C. Evaluation of hepatocellular carcinoma using SonoVue, a second generation ultrasound contrast agent: correlation with cellular differentiation. *Eur Radiol* 2004; **14**: 1092-1099
29 **Bruix J**, Sherman M, Llovet JM, Beaugrand M, Lencioni R, Burroughs AK, Christensen E, Pagliaro L, Colombo M, Rodés J. Clinical management of hepatocellular carcinoma. Conclusions of the Barcelona-2000 EASL conference. European Association for the Study of the Liver. *J Hepatol* 2001; **35**: 421-430
30 **Bruix J**, Sherman M. Management of hepatocellular carcinoma. *Hepatology* 2005; **42**: 1208-1236

S- Editor Liu Y **L- Editor** Kumar M **E- Editor** Bai SH